Journal of Applied Science and Environmental Studies
JASES
http://revues.imist.ma/index.php?journal=jases

Original Paper

THEORETICAL STUDY OF 2-METHYL BENZOAZOLE AND ITS DERIVATIVES AS CORROSION INHIBITORS ON ALUMINIUM METAL SURFACE

A. M. AYUBA*, T. A. NYIJIME

Department of Pure and Industrial Chemistry, Faculty of Physical Sciences, Bayero University, Kano, Nigeria

* Corresponding author. E-mail address: ayubaabdullahi@buk.edu.ng

Received 16 February 2021; Revised 06 July 2021, Accepted 30 August 2021

Keywords
Electronic properties
Binding energy
Molecular dynamics
Quatum parameters
Local reactivity

Abstract

Corrosion inhibition efficiency potentials of 2-methyl benzoazole and its derivatives on Aluminium metal were studied through the evaluation of their quantum chemical parameters and molecular dynamics simulations approaches. Quantum chemical parameters were used to calculate the electronic properties of the inhibitor molecules in order to correlate their inhibition with their molecular structure. The quantum chemical parameters include : E_{HOMO} (Highest occupied molecular orbital energy), E_{LUMO} (Lowest unoccupied molecular orbital energy), energy gap (ΔE), dipole moment (μ), global hardness (η), global softness (σ), the absolute electronegativity (χ) and the fractions of electrons transferred (ΔN) from the molecules to the metal. Furthermore, the local reactivity of the molecules was analyzed through the Fukui functions and found to be located on the molecule's heteroatoms (sulphur, oxygen, nitrogem and selenium). The molecular dynamic simulation results showed that the adsorption energy is low, negative and within the threshold of physical adsorption mechanism. The order of inhibition efficiency of the studied 2-methyl benzoazole and its derivatives on Aluminium metal is 2-MBT>2-MBS>2-MBI>2-MBX>2-MBA.

1. Introduction

Corrosion inhibition is a popular method used in minimizing, preventing and protecting corrosion of metal surfaces subjected to deleterious corrosive environments including acidic, alkaline among others [1-2]. Based on their physical, chemical and aesthetic properties, many metals have found industrial applications involving chemical materials, petrochemical installments, paper industries,

pollution control settings, hydrometallurgy and petroleum industries, ships and aerospace manufacture among others [3]. Aluminium is one of the most abundant metals on earth and has find lots of industrial applications. This metal is known to resist corrosive environments to some extent due to the thin film of protective oxide it possesses which is usually depleted when it is in contact with severe corrosive agents, and therefore the need to protect this metal from corrosive destruction. By adding small concentration of inhibitors to corrosive environments, the extent of the reaction of this metal with the corrosive media is greatly minimized [4-8]. These inhibitors are established to reduce the corrosion rate of aluminium through a mechanism believed to involve either changing the anodic or cathodic reaction, reducing diffusion rate of reactants onto the metal surface or forming a protecting layer on the metal surface [9].

Experimental techniques have been used to explain the inhibition mechanism, but they are often time consuming and expensive and therefore, the need to search for alternative methods. The advancement in computer software and hardware engineering has provided powerful use of theoretical modeling techniques which successfully correlate the inhibition efficiency of the inhibitors with their molecular structure and properties [10-15]. In most situations, parameters connected with the electronic and the chemical structure of the molecule act simultaneously on the inhibitor efficiency and therefore difficult to decide which parameter plays the most important role in increasing the inhibitor efficiency [16-18]. Adsorption characteristics of these inhibitors depend on several factors including the nature and number of potential adsorption sites present in the inhibitor molecule. Different attempts are made to link the corrosion inhibitor efficiency with a number of structural parameters of these molecules [19-23]. For this reason, organic compounds which have similar structures were chosen in this investigation. It is assumed that, the influence of the chemical structure will be very similar and the influence of the electronic structure can be clearly investigated.

The choice of these compounds based on molecular structure considerations, i.e. these are organic substances with almost similar chemical structure, is expected to help in establishing the differences in the inhibition properties mainly due to the difference in electronic structure of these compounds.

This work is aimed at theoretically studying the inhibition efficiency of 2-methyl benzoazole and its derivatives (Figure 1) and to correlate these efficiencies with the quantum chemical parameters of the investigated compounds. The calculated quantum chemical parameters are the highest occupied molecular orbital (E_{HOMO}), lowest unoccupied molecular orbital (E_{LUMO}), separation energy (ΔE), dipole moment (μ), and those parameters that give valuable information about the reactive behaviour such as the electronegativity (χ), the ionization potential (I), the hardness (η), the softness (σ), and the fraction of electrons transferred from the inhibitor molecule to the metal surface (ΔN). Furthermore, the interaction energies of the investigated inhibitors on the aluminum surface were also evaluated to be able to correlate them with that reported by Al-Mayouf *et al*. [59] who studied experimentally the inhibition efficiences of these compounds (2-methylbenzoazole and its derivatives) on 304SS.

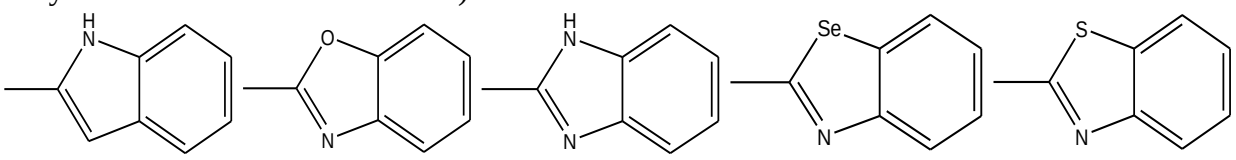

2-methylbenzoazole 2-methylbenzoxazole 2-methylbenzoimidazole 2-methylbenzoselenazole 2-methylbenzothiazole

Figure 1. Molecular Structures of 2-methyl benzoazole derivatives

2. Experimantal Details

All the geometries of the 2-methyl benzoazole and its derivatives were fully optimized using the B3LYP method within the framework of density functional theory (DFT), electronic structure programs, $DMol^3$ as contained in the Materials Studio 7.0 software (Accelrys, Inc.) [24-25]. Following the geometry optimizations, analytical frequency calculations were performed at the DFT/6-311G (d, p) level using standard procedures to obtain the thermochemical properties. All these calculations were carried out on a HP Pavilion personal computer with an installed Material studio program package [26]. These calculations have been widely used to study reaction mechanisms [27] and have also been proved to be a very powerful tool for studying inhibition of the corrosion of metals [28-29]. Recently, density functional theory (DFT) has been used to analyze the characteristics of the inhibitor/metal surface mechanisms and to describe the structural nature of the inhibitor in the corrosion inhibition process [30].

For closed-shell molecules, ionization potential (IP) and electron affinity (EA) can be expressed in terms of E_{HOMO} (highest occupied molecular orbital energy) and E_{LUMO} (lowest unoccupied molecular orbital energy) using equations (1) and (2) respectively [31]:

$$IP = -E_{HOMO} \quad (1)$$

$$EA = -E_{LUMO} \quad (2)$$

Calculated values of IP and EA were used to determine the values of the absolute electronegativity χ, the global hardness (η) and the global softness (σ) using equations (3), (4) and (5) [32]:

$$\chi = \frac{(IP+EA)}{2} = \frac{E_{LUMO}+E_{HOMO}}{2} \quad (3)$$

$$\eta = \left(\frac{IP-EA}{2}\right) = \frac{E_{LUMO}-E_{HOMO}}{2} \quad (4)$$

The global softness (σ) is the inverse of the global hardness [32].

$$\sigma = 1/\eta \quad (5)$$

However, for a reaction of two systems with different electronegativities, the electronic flow occur from the molecule with the lower electronegativity (the organic inhibitor) towards that of a higher value (metallic surface) till both chemical potentials are equal [33]. Therefore, the fraction of electrons transferred (ΔN) from the inhibitor molecule to the metallic atoms was calculated according to Pearson electronegativity scale using equation (6) [34]:

$$\Delta N = \frac{\chi_{Al}-\chi_{inh}}{2(\eta_{Al}+\eta_{inh})} \quad (6)$$

Where χ_{Al} and χ_{inh} denote the absolute electronegativity of aluminium and the inhibitor molecule, respectively, and η_{Al} and η_{inh} denote the absolute hardness of aluminium and the inhibitor molecule respectively. To calculate the fraction of electrons transferred, a theoretical value for the electronegativity of bulk aluminium was used, χ_{Al} = 5.60 eV [35], and a global hardness of η_{Al} = 0, by assuming that for a metallic bulk IP = EA, because they are softer than the neutral metallic atoms [36-37]. The reactive sites on the inhibitor molecules were analyzed through evaluation of their Fukui indices [38]. The Fukui indices are measures of chemical reactivity, as well as an indicative of the reactive regions and the nucleophilic and electrophilic behaviour of the molecule. Regions of a molecule where the Fukui function is large are chemically softer than regions where the Fukui function is small, and by invoking the hard and soft acids and bases (HSAB) principle in a local sense, one may establish the behaviour of the different sites with respect to hard or soft

reagents. The Fukui function f(r) is defined as the first derivative of the electronic density q(r) with respect to the number of electrons N at constant external potential v(r). Thus, using a scheme of finite difference approximations from Mulliken population analysis of atoms in the 2-methyl benzoazole and its derivatives, depending on the direction of electron transfer from equation (7) for nucleophilic attack and (8) for nucleophilic attack [39-42]:

$$f_k^+ = q_{k(N+1)} - q_{k(N)} \quad (7)$$

$$f_k^- = q_{k(N)} - q_{k(N-1)} \quad (8)$$

Where q_k is the gross charge of atom k in the molecule, i.e., the electron density at a point r in space around the molecule. N corresponds to the number of electrons in the molecule. N + 1 corresponds to an anion, with an electron added to the LUMO of the neutral molecule; N - 1 corresponds to the cation with an electron removed from the HOMO of the neutral molecule. All calculations were done at the ground state geometries [37].

Molecular dynamics (MD) simulation of the interaction between a single molecule and the Al surface was performed using Forcite quench MD in Material Studio (MS) Modeling 7.0 software to sample many different low-energy minima and to determine the global energy minimum [36] [41-42]. Calculations were performed on a 9 x 7 supercell using the condensed-phase optimized molecular potentials for atomistic simulation studies (COMPASS) force field and the Smart algorithm. Al (1 1 0) surface used is the most densely packed and also the most stable [40-44]. The Al crystal was cleaved along the (1 1 0) plane. The Al slab built for the docking process was significantly larger than the inhibitor molecules in order to avoid edge effects during docking. Temperature was fixed at 350 K, with NVE ensemble, with time step of 1fs and simulation time of 5 ps. The system was quenched every 250 steps with the Al (1 1 0) surface atoms constrained. Optimized structure of each inhibitor molecule was used for the simulation. Adsorption of a single 2-methyl benzoazole derivatives onto the Al (1 1 0) surface provides access to the adsorption energetics and its effect on the inhibition efficiency each molecule. Thus, the adsorption (E_{ads}) and binding ($E_{binding}$) energies between the inhibitor molecules and Al (1 1 0) surface was calculated using equation (9) [40-44]:

$$E_{Binding} = -E_{Ads} = E_{complex} - (E_{inhibitor} + E_{Al\ surface}) \quad (9)$$

Where $E_{complex}$ is the total energy of the Al surface and inhibitor, $E_{Alsurface}$ is the energy of the Al surface without the inhibitor, and $E_{inhibitor}$ is the energy of the inhibitor without the Al surface.

3. Results and Discussion

3.1 Quantum chemical parameters

Quantum chemical parameters and simulation molecular dynamics were performed to determine the electronic structures of the molecules of the 2-methyl benzoazole and its derivatives in order to establish the active sites as well as local reactivities of the molecules.

Figures 1 shows the geometric optimized structure, the total electron density, highest occupied molecular orbital (HOMO) and lowest unoccupied molecular orbital (LUMO) of 2-methyl benzoazole (2-MBA, the reference molecule), whereas Figures 2 shows similar structures of 2-methyl benzoselenazole (2-MBS), Figure 3, 2-methyl benzothiazole (2-MBT), Figure 4, 2-methyl benzoxazole (2-MBX) and Figure 5, 2-methyl benzoimidazole (2-MBI) respectively. The electron density is saturated all around each molecule; which facilitate flat-lying adsorption orientations of the molecules [45]. The regions of high HOMO density are the sites at which electrophiles attack

and represent the active centers, with the outmost ability to bond to the metal surface, whereas the LUMO orbital are accept the electrons in the p- or d-orbital of the metal using antibonding orbitals to form feedback bonds [45-47]. It can be observed that the HOMO orbital for 2-methyl benzoselenazole (2-MBS) and 2-methyl benzothiazole (2-MBT) is saturated around the selenium and amine functional group, whereas for 2-methyl benzoazole (reference molecule), 2-methyl benzoxazole (2-MBX) and 2-methyl benzoimidazole (2-MBI) the HOMO orbitals are saturated on the nitrogen, oxygen, sulfur atoms respectively while the LUMO orbital is around the carbonyl atoms. The trend of HOMO–LUMO locations is common to all 2-methyl benzoazole and its derivatives which could lead to high similarities in their adsorption characteristics.

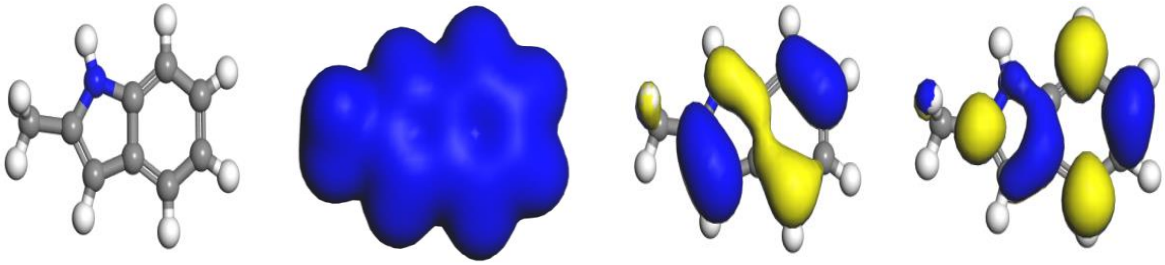

(a) **(b)** **(c)** **(d)**

Figures 1. Structural and electronic properties of 2-methyl benzoazole (2-MBA) (a) Optimized geometry (b) Total electron density (c) Highest occupied molecular orbital (d) Lowest unoccupied molecular orbital (reference molecule)

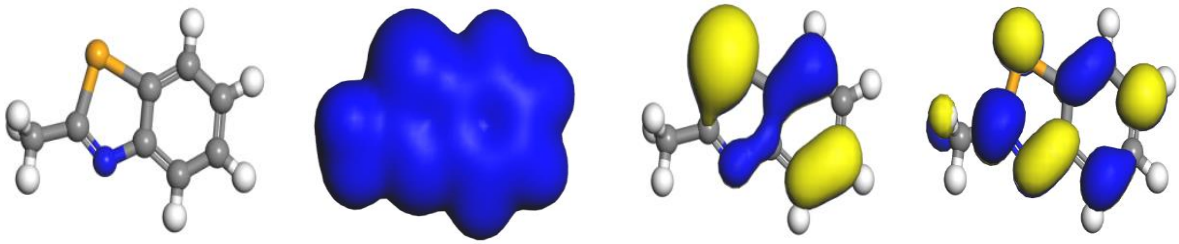

(a) **(b)** **(c)** **(d)**

Figures 2. Structure and electronic properties of 2-methyl benzoselenazole (2-MBS) (a) Optimized geometry (b) Total electron density (c) Highest occupied molecular orbital (d) Lowest unoccupied molecular orbital

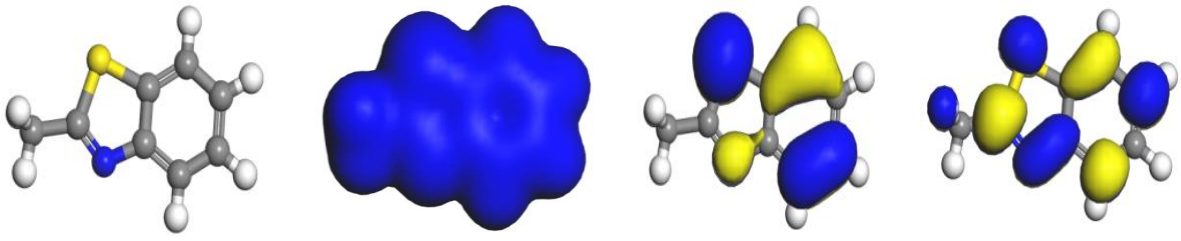

(a) **(b)** **(c)** **(d)**

Figures 3. Structure and electronic properties of 2-methyl benzothiazole (2-MBT) (a) Optimized geometry (b) Total electron density (c) Highest occupied molecular orbital (d) Lowest unoccupied molecular orbital.

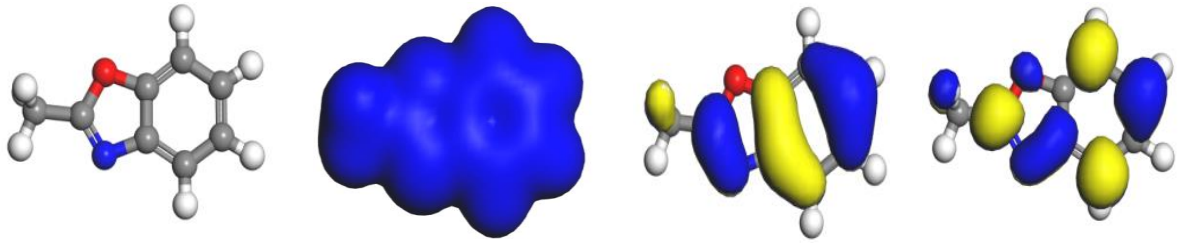

(a) **(b)** **(c)** **(d)**

Figures 4. Structure and Electronic Properties of 2-methyl benzoxazole (2-MBX) (a) Optimized Geometry (b) Total Electron Density (c) Highest Occupied Molecular Orbital (d) Lowest Unoccupied Molecular Orbital

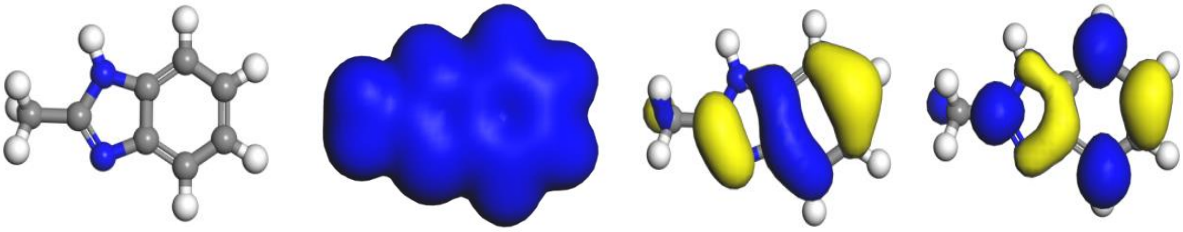

(a) **(b)** **(c)** **(d)**

Figures 5. Structure and electronic properties of 2-methyl benzoimidazole (2-MBI) (a) Optimized geometry (b) Total electron density (c) Highest occupied molecular orbital (d) Lowest unoccupied molecular orbital

Some other quantum chemical parameters related to the molecular and electronic structures of the most stable conformation of the molecules after geometric optimizations are presented in Table 1. High values of E_{HOMO} indicate the disposition of the molecule to donate electrons to an appropriate acceptor with vacant molecular orbitals, whereas low values of ΔE will favor good inhibition efficiencies, because the energy to remove an electron from the last occupied orbital will be minimized [46-47]. The reference molecule (2-methyl benzoazole) has least value of ΔE relative to its derivatives. The obtained values presented in Table 1 showed that all the molecules have comparable E_{HOMO} values, which is not very surprising because the functional groups that comprise the HOMO are similar. Higher values of dipole moment are usually characterized to be associated with good inhibition properties [48-51]. The dipole moment calculated for all the molecules are relatively close, with the reference molecule having the lowest value while the direction of their dipoles is similar and they are projected to the molecular plane. The direction of dipole can be understood by considering the electrostatic potential, which discerns electron density rich regions centered on the carbon, amine indicating the preferred zone for electrophilic attack. Dipole moments are substantially enhanced for both inhibitors on going from the gaseous to the aqueous phase, indicating an increase in the stability of the inhibitors due to the interaction with water [52]. Considering all these factors, a clear trend was observed for the studied molecules in respect of increase in E_{HOMO} values, decrease in ΔE values and decrease in dipole moment.

Similarly, some other electronic and structural quantum chemical parameters of the studied inhibitors are also presented in Table 1. These include their; ionization potential, electron affinity, absolute (global) hardness, global softness, absolute electronegativities and fraction of electron transferred respectively. The number of electrons transferred from the molecule to metal ΔN, was calculated, where aluminium is considered as Lewis acid according to hard-soft acid and bases

(HSAB) concept [52]. The difference in electronegativity between the inhibitor and the aluminium drives the electron transfer, and the sum of the hardness parameters acts as a resistance. If ΔN is less than 3.6, inhibition efficiency increases with increasing values of the electron donating ability of the molecules, while values of ΔN greater than 3.6 indicate a decrease in inhibition efficiency with increase in electron donating ability of the inhibitor [53-55]. The earlier case is found to be applicable to all the studied molecules since their ΔN values are all less than 3.6.

Table 1. Computed Quantum Chemical Parameters (Electronic and Structural) of the Studied Inhibitor Molecules

	Inhibitors				
Properties	**2-MBA**	**2-MBS**	**2-MBT**	**2-MBX**	**2-MBI**
HOMO (at orbital number)	35	96	78	70	70
LUMO (at orbital number)	36	97	79	71	71
E_{HOMO} (eV)	-5.686	-6.553	-6.704	-6.697	-6.338
E_{LUMO} (eV)	-0.499	-1.342	-1.248	-0.999	-0.700
ΔE (eV)	5.187	5.211	5.456	5.698	5.638
Dipole moment (debye)	3.018	3.380	3. 620	3.438	3.283
Ionization potential (I) (eV)	5.686	6.553	6.704	6.697	6.338
Electron affinity (A) (eV)	0.499	1.342	1.248	0.999	0.700
Global hardness (η)	2.594	2. 606	2.728	2.849	2.819
Global softness (σ)	0.386	0.384	0.367	0.351	0.355
Absolute electronegativity (χ)	3.093	3.948	3.976	3.848	3.519
Fraction of electrons transferred (ΔN)	0.483	0.317	0.298	0.307	0.369

3.2 Local reactivity (Fukui indices) determination

The local reactivity of each molecule was analyzed by means of the Fukui indices (FI) to assess reactive centers in terms of their nucleophilic and electrophilic behaviours. This is to distinguish each part of the molecule on the basis of its distinct chemical behaviour due to different functional groups or substituents. The f^+ is a measure of reactivity relating to nucleophilic attack or tendency of the molecule to attract electrons, whereas, f^- measures reactivity with respect to electrophilic attack of the molecule to release electrons. The values obtained for 2-methyl benzoazole and its derivatives were summarized in Table 2. In the nucleophilic (f^+), 2-methyl benzoazole (2-MBA) have its highest Mulliken and Hirshfeld charges on C(6), C(9) atom, 2-methyl benzoselenazole (2-MBS), have it on Se(1) and C(2) atom, 2-methyl benzothiazole (2-MBT) have its own on S(1), C(2) and N(3), 2-methyl benzoxazole (2-MBX) has its own on C(2, 9, 6) and 2-methyl benzoimidazole (MBI) has its own on C(6, 9) respectively. While for the electrophilic (f^-), 2-methyl benzoazole (2-MBA) have its highest Mulliken charge on C(3, 8) and Hirshfeld charge on C(3, 8), 2-methyl benzoselenazole (2-MBS) on Se(1) and C(9), 2-methyl benzothiazole (2-MBT) on S(1), C(9, 6) and S(1), 2-methyl benzoxazole (2-MBX) on C(2, 4, 8), 2-methyl benzoimidazole (2-MBI) have on N(2), C(8). The similarities in quantum chemical parameters show that the adsorption strengths of the molecules would be mostly determined by molecular size parameters rather than electronic structure parameters alone [55].

Table 2. Calculated Fukui Indices for the Studied Inhibitor Molecules

	Nucleophilic (f^+)		Electrophilic (f^-)	
	Mulliken	**Hirshfield**	**Mulliken**	**Hirshfield**
Molecule	**Atom Value**	**Atom Value**	**Atom Value**	**Atom Value**
2-methyl benzoazole	C(6) 0.156	C(6) 0.128	C(3) 0.150	C(3) 0.145
(2-MBA)	C(9) 0.148	C(8) 0.096	C(8) 0.084	C(8) 0.093
2methylbenzoselenazole	Se(1) 0.229	Se(1) 0.197	Se(1) 0.349	Se(1) 0.322
(2-MBS)	C(2) 0.125	C(2) 0.121	C(9) 0.081	C(9) 0.083
2-methyl benzothiazole	S(1) 0.173	S(1) 0.155	S(1) 0.173	S(1) 0.246
(2-MBT)	C(2) 0.131	C(2) 0.125	C(6) 0.103	C(6) 0.106
	N(3) 0.079	N(3) 0.089	C(9) 0.111	C(9) 0.113
2-methyl benzoxazole	C(2) 0.125	C(2) 0.113	C(2) 0.094	C(2) 0.085
(2-MBX)	C(6) 0.138	C(6) 0.105	C(4) 0.125	C(4) 0.102
	C(9) 0.117	C(9) 0.114	C(8) 0.086	C(8) 0.141
2-methylbenzoimidazole	C(6) 0.154	C(6) 0.127	N(2) 0.090	N(2) 0.094
(2-MBI)	C(9) 0.147	C(9) 0.124	C(8) 0.095	C(8) 0.113

3.3 Molecular dynamics simulations

Adsorption of each inhibitor molecule on the aluminium metal surface was performed at a molecular level by molecular simulation dynamics method using Forcite quench molecular dynamics. This is to display many different low energy configurations and to identify the low energy minima. Figures 6 shows representative snapshots of the side view of the lowest energy adsorption configurations for single molecule of 2-methyl benzoazole (2-MBA) and its derivatives respectively on the Al (110) surface from the simulations processes. Each molecule can be seen to maintain flat lying adsorption orientation on the Al surface, as expected from the delocalization of the electron density all around the molecules. This orientation maximizes contact with the metal surface and hence auguments their degree of surface coverage. This parallel adsorption orientation also facilitates interaction of π - electrons of the hetero-atoms (Se, S and N) in the molecules with the aluminium metal surface. A detailed analysis of the adsorbed molecules on Al (110) showing the soft epitaxial adsorption mechanism with accommodation of the molecular backbone in characteristic epitaxial grooves on the aluminium metal surface are showed in Figures 6. The adsorption reveals a very clear trend in the adsorption configuration in which polarizable atoms along the molecular backbone appear to align with vacant sites on the face-centered cubic lattice on top of the aluminium metal surface. Such epitaxial adsorption configuration, which is associated with a minimum free energy of adsorption, has also been reported for some compounds and this accounts for the stable adsorption structures [45-56].

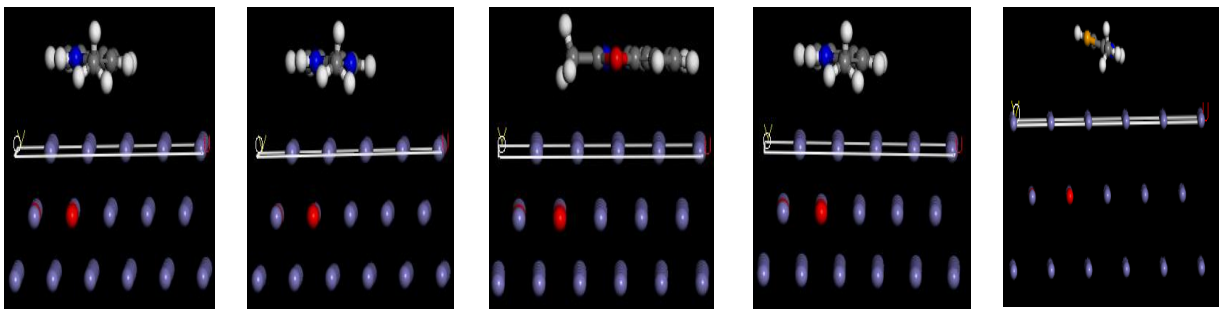

2-MBA **2-MBX** **2-MBI** **2-MBS** **2-MBT**

F**igures 6.** Side view snap shot of the adsorbed single a) 2-MBA b) 2-MBX c) 2-MBI d) 2-MBS e) 2-MBI molecules on Aluminium (110) surface

To quantitatively appraise the interactions between each molecule and the aluminium surface, the adsorption energies (E_{ads}) and binding energies (E_{bind}) were calculated. A negative value of E_{ads} corresponds to a stable adsorption structure. The total energies were calculated by averaging the energies of the five most stable (lowest) representative adsorption configurations and the results were presented in Table 6. The obtained E_{ads} values; $-60.63\pm2.9\times10^{-5}$ kcal/mol for MBI, $-59.42\pm1.1\times10^{-5}$ kcal/mol for MBX, $-58.72\pm4.4\times10^{-2}$ kcal/mol for MBA, $-60.63\pm2.4\times10^{-5}$ kcal/mol for MBS and $-71.02\pm3.1\times10^{-2}$ kcal/mol for MBT were all negative and of relatively low magnitude, suggesting stable adsorption structures [58]. This low affinity of the inhibitors for the aluminium surface may account for the experimentally relatively low corrosion inhibition efficacy of the molecules reported by Al-Mayouf *et al*. [59]. However, the magnitudes of the calculated binding energies were all less than 100 kcal mol^{-1} (Table 3). This is despite the fact that the simulations did not take into consideration the specific covalent interactions between the molecules and the aluminium surface. This value has been reported to be in the range of physisorptive interactions [48, 55, 61]. It has also been reported that the more positive the binding energy of the inhibitor-metal surface is, the better the adsorption of the inhibitor onto the metal surface and subsequently the higher the inhibition efficiency [46, 52, 57-58].

Table 3. Calculated adsorption parameters for the interaction of the studied molecules with the Al(110) surface using Forcite quench dynamics

Molecules	**E_{Comp}** kcal/mol	**E_{Inh}** kcal/mol	E_{Al}kcal/mol	**E_{Ads}** kcal/mol	**E_{Bin}** kcal/mol
2-MBI	$47.41\pm3.7\times10^{-10}$	$108.04\pm2.9\times10^{-5}$	0.00 ± 0.00	$-60.63\pm2.9\times10^{-5}$	$60.61\pm2.9\times10^{-5}$
2-MBX	$-20.95\pm6.8\times10^{-10}$	$38.47\pm1.1\times10^{-5}$	0.00 ± 0.00	$-59.42\pm1.1\times10^{-5}$	$59.42\pm1.1\times10^{-5}$
2-MBA	$-48.36\pm7.0\times10^{-9}$	$10.36\pm4.4\times10^{-2}$	0.00 ± 0.00	$-58.72\pm4.4\times10^{-2}$	$58.72\pm4.4\times10^{-2}$
2-MBS	$47.41\pm9.9\times10^{-10}$	$108.04\pm2.4\times10^{-5}$	0.00 ± 0.00	$-60.63\pm2.4\times10^{-5}$	$60.63\pm2.4\times10^{-5}$
2-MBT	$49.34\pm5.4\times10^{-8}$	$121.05\pm3.1\times10^{-2}$	0.00 ± 0.00	$-71.02\pm3.1\times10^{-2}$	$71.02\pm3.1\times10^{-2}$

Conclusion

The following main conclusions are drawn from the present study:

➢Quantum chemical parameters associated with the electronic structures of the inhibitor molecules showed that their inhibiting potentials follow the order: 2-MBT>2-MBX>2-MBS>2-MBI>2-MBA.

➢The local reactivities through Fukui indices showed that the point of association of the inhibitor molecules with the aluminium surface is through their heteroatoms of nitrogen, oxygen, sulfur or selenium respectively.

➢The calculated adsorption/binding energy values obtained were negative and low, signifying low adsorption and inhibition with a proposed mechanism of physical adsorption.

➢Molecular dynamic simulations of a single inhibitor molecule on aluminium surface show the order of inhibition efficiency: 2-MBT>2-MBS>2-MBI>2-MBX>2-MBA.

References

1. A. Doner, R. Solmaz, M. Ozcan, J. Gu, Experimental and theoretical of thiazoles as corrosion inhibitors for mild steel in sulphuric acid solution, **Corrosion Science,** 53 (9) (2011) 2902-2913.
2. M. Abdallah, Rhodanineazosulpha drugs as corrosion inhibitors for corrosion of 304 stainless steel in hydrochloric acid solution, **Corrosion Science,** 44 (4) (2002) 717-718.
3. F. Gapsari, W. Suprapto, R. Soenoko, A. Suprato, The inhibition of 304SS in hydrochloric acid solution by cera alba extract, **Journal of engineering science and technology**, 12(8) (2017) 2078-2090.
4. A.Y. EL-Etre, Natural honey as corrosion inhibitor for metals and alloys. I. Copper in neutral aqueous solution. **Corrosion Science,** 40(11) (1998) 1845-1850.
5. J. L.Wang, P. H. Luo, Corrosion inhibition of zinc in phosphoric acid solution by 2-mercaptobenzimidazole, **Corrosion Science,** 45(4) (2003) 677-683.
6. S. Garai, S. Garai, S. Parasuraman, S. Jaisankar, J. K. Singh, A. Elango, A comprehensive study on crude ethanolic extract of Artemisia pallens (Asteraceae) and its active component as effective corrosion inhibitors of mild steel in acid solution. **Corrosion Science,** 60 (2012) 193-204.
7. P. B. Raja, M. G. Sethuraman, Natural products as corrosion inhibitor for metals incorrosive media, Review**, Materials Letter**, 62(1) (2008) 113-116.
8. K. I. Radojcˇic, S. Berkovic´, J. Kovac, F. Vorkapic, Natural honey and black radish juice as tin corrosion inhibitors. *Corrosion Science*, **Corrosion Science, 50(5)** (2009) 1498-1504.
9. P. R. Roberge, Handbook of corrosion Engineering. New York: McGraw Hill, 2000.
10. M. S. Masoud, M. K. Awad, M. A. Shaker, M. M. T. El-Tahawy, The role of structural chemistry in the inhibitive performance of some aminopyrimidines on the corrosion of steel, **Corros. Sci**, 52 (2010) 2387-2394.
11. H. J. Henriquez-Roman, L. Padilla-Campos, M. A. Paez, J. H. Zagal, M. A. Rubio, C. M. Rangel, J. Ostamagna, G. Cardenas-Jiron, The influence of aniline and its derivatives on the corrosion behaviour of copper in acid solution: a theoretical approach, **J. Mol. Struct.** *(THEOCHEM)*, 757 (2005) 1-12.
12. N. Khalil, Quantum chemical approach of corrosion inhibition, **Electrochim. Acta,** 48 (2003) 2635-2642.
13. M. Behpour, S. M. Ghoreishi, N. Soltani, M. Salavati-Niasari, M. Hamadanian, A. Gandomi, Electrochemical and theoretical investigation on the corrosion inhibition of mild steel by thiosalicylaldehyde derivatives in hydrochloric acid solution, **Corros. Sci.,** 50 (2008) 2172-2179.
14. M. K. Awad, R. M. Issa, F. M. Atlam, theoretical investigation of the inhibition of corrosion by some triazole Schiff bases, **Mater. Corros.** 60 (2009) 813-819.

15. M. K. Awad, Semiempirical investigation of the inhibition efficiency of thiourea derivatives as corrosion inhibitors, **J. Electroanal. Chem. 567 (2004) 219-227.**
16. K. F. Khaled, M. M. Al-Qahtani, The inhibitive effect of some tetrazole derivatives toward Al corrosion in acid solution. Chemical, electrochemical and theoretical studies, **Materials Chemistry and Physics,** 113 (2009) 150–158.
17. A. Popova, M. Christov, T. Deligeorgiev, AC and DC study of the temperature effect on mild steel corrosion in acid medium in the presence of benzimidazole derivatives, **Corrosion Sci**, 59 (2003) 756-760.
18. A. Popova, M. Christov, S. Raicheva, E. Sokolova, adsorption characteristic of corrosion inhibitors from corrosion rate measurement, **Corros. Sci.**, 46 (2004) 1333-1345.
19. W. Yang, W. J. Mortier, The use of global and local molecular parameters for the analysis of the gas-phase basicity of amine, **J. Am. Chem. Soc**., 108 (1986) 5708-5711.
20. C.Vermaa, M. A. Quraishia, L. B. Olasunkanmib, E. E. Ebenso, Substituents effect on corrosion inhibition performance of organic compounds in aggressive ionic solutions. A review, **Royal Society of Chemistry (Advances),** (2018)1-52.
21. V. M. Udowo, I. E. Uwah, F. E. Daniel, F. Abeng, S. Ivara, Computational and experimental study of the inhibition effects of purple sweet potato leaves extract on mild steel corrosion in 1M H_2SO_4 **Journal of Physical Chemistry & Biophysics** 7(3) (2017) 1-6.
22. K. Rasheeda, D. P. Vijaya, P. A. Alva, Krishnaprasad, S. Samshuddin, Pyrimidine derivatives as potential corrosion inhibitors for steel in acid medium-An overview, **Int. J. Corros. Scale Inhib.**, 7(1) 201848–61.
23. N. O. Obi-Egbedi, N. D. Ojo, Computational studies of the corrosion inhibition potentials of some derivatives of 1H-Imidazo [4, 5-F] [1, 10] phenanthroline, **Journal of Science Research,** 14 (2015) 50-56.
24. A. D. Becke, Density-functional thermochemistry. III. The role of exact exchange, **J ChemPhys**, 8 (1993) 5648-5653.
25. Lee, W. Yang and R.G. Parr. Development of the Colle-Salvetti correlation-energy formula into a functional of the electron density, **Phys Rev B**, 37 (1988) 785-793.
26. M. J. Frisch, G. W. Trucks and H. B. Schlegel, Gaussian 09, Rev. A. 1 Gaussian, Inc., Wallingford CT, 2009.
27. Z. Tao, S. Zhang, W. Liand B. Hou, Adsorption and corrosion inhibition behavior of mild steel by one derivative of benzoic−triazole in acidic solution, **Ind. Eng. Chem. Res.,** 49 (2010) 2593-2599.
28. K. C. Emregul, M. Hayvali, Studies on the effect of a newly synthesized Schiff base compound from phenazone and vanillin on the corrosion of steel in 2 M HCl, **Corros. Sci.,** 48 (2006) 797-812.
29. K. F. Khaled, K. Babic-Samardzija and N. Hackerman, Theoretical study of the structural effects of polymethylene amines on corrosion inhibition of iron in acid solutions, **Electrochim. Acta**. 50 (2005) 2515-2520.
30. M. Lashkari and M. R. Arshadi, DFT studies of pyridine corrosion inhibitors in electrical double layer: solvent, substrate, and electric field effects, **Chem J. Chem. Phys.,** 299 (2004) 131-137.

31. T. Koopmans, Ordering of wave functions and eigenergies to the individual electrons of an atom, **Physica,** 1 (1993) 104-113.
32. R. G. Pearson, Hard and soft acids and bases, **J. Am. Chem. Soc,** 22 (1963) 3533-3539.
33. R. G. Parr, L. Szentpaly and S. Liu. Electrophilicity index, **J. Am. Chem. Soc,** 121 (1999) 1922-1924.
34. K. F. Khaled, Studies of iron corrosion inhibition using chemical, electrochemical and computer simulation techniques, **Electrochim. Acta,** 22 (2010) 6523.
35. F. L. Hirshfeld, A novel definition of a molecule in a crystal, **Theor. Chem. Acc.** 44 (1977) 129–138.
36. P. Zhao, Q. Liang, Y. Li, Electrochemical, SEM/EDS and quantum chemical study of phthalocyanines as corrosion inhibitors for mild steel in 1 mol/l HCl, **J. Applied Surface Science**, 252(5) (2005) 1596-1607.
37. W. Yang, W. J. Mortier, The use of global and local molecular parameters for the analysis of the gas-phase basicity of amine, **J. Am. Chem. Soc.,** 108 (1986) 5708-5711.
38. V. M. Udowo, I. E. Uwah, F. E. Daniel, F. Abeng, S. Ivara, Computational and experimental study of the inhibition effects of purple sweet potato leaves extract on mild steel corrosion in 1M H_2SO_4, **J. of Physical Chemistry & Biophysics** 7 (2017) 1-6.
39. K. Rasheeda, D. P. Vijaya, P. A. Alva, Krishnaprasad, S. Samshuddin, Pyrimidine derivatives as potential corrosion inhibitors for steel in acid medium-An overview, **Int. J. Corros. Scale Inhib.,** 7 (2018) 48–61
40. N. O. Obi-Egbedi, N. D. Ojo, Computational studies of the corrosion inhibition potentials of some derivatives of 1H-Imidazo[4,5-F] [1,10] phenanthroline, **J. of Science Research**, 14 (2015) 50-56.
41. H. Zhao, X. Zhang, L. Ji, H. Hu, Q. Li, Quantitative-activity relationship model for amino acids as corrosion inhibitors based on the support reactor machine and molecular design, **Corrosion Science**, 2 (2014) 11-23.
42. A. Mishra, C. Verma, V. Srivastava, H. Lgaz, M. A. Quraishi, E. E. Ebenso, M. Chung, Synthesis, characterization and corrosion inhibition studies of N-phenyl-benzamides on the acidic corrosion of mild steel. Experimental and computational studies, **J. of Bio- and Tribo-Corrosion**, 2018, 4-32.
43. H. Lgaz, R. Salghi, A. Chaouiki, Shubhalaxmi, S. Jodeh, K. S. Bhat, Pyrazoline derivatives as possible corrosion inhibitors for mild steel in acidic media: A combined experimental and computational approach, **Cogent Engineering**, 5*(*2018) 1441585.
44. G. Gece and S. Bilgic, Quantum chemical study of some cyclic nitrogen compounds as corrosion inhibitors of steel in NaCl media, **Corros Sci.,** 51 (2009) 1876-1878.
45. E. E. Oguzie, C. B. Adindu, C. K. Enenebeaku, C. E. Ogukwe, M. A. Chidiebere, L. L. Oguzie, Natural products for materials protection: Mechanism of corrosion inhibition of mild steel by acid extracts of *Piper guineense*, **Journal of Physical Chemistry**, **2012**, dx.doi.org/10.1021/jp300791s.
46. O. Akalezi, C. E. Ogukwe, C. K. Enenebaku, E. E. Oguzie, Application of aqueous extracts of coffee senna for control of mild steel corrosion in acidic environments, **Environment and Pollution**, 1, 2 (2012) 45-60.

47. A. K. Singh, M. A. Quraishi, Inhibiting effects of some 5-substituted isatin-based mannich bases on the corrosion of mild steel in hydrochloric acid solution, **Journal of Applied Electrochemistry,** 40, 7 (2010) 1293-1306.
48. M. A. Ameer, A. M. Fekry, Inhibition effect of newly synthesized heterocyclic organic molecules on corrosion of steel in alkaline medium containing chloride, **International Journal of Hydrogen Energy,** 35, 20 (2010) 11387-11396.
49. W. Li, L. Hu, Z. Tao, H. Tian, B. Hou, Experimental and quantum chemical studies on two triazole derivatives as corrosion inhibitors for mild steel in acid media, **Material Corrosion,** 62, 11 (2011) 1042-1050.
50. S. John, J. Joy, M. Prajila, A. Joseph, Adsorption and inhibition effect of methyl carbamate on copper metal in 1N HNO_3. An experimental and theoretical study, **Material Corrosion,** 62, 11 (2011) 1031-1041.
51. S. M. A. Hosseini, M. J. Bahrami, A. Dorehgiraee, Inhibition investigation and determination of some quantum chemical parameters of 1-(4-(dimethylamino) benzylidene) thiosemicarbazide on steel alloys in sulfuric acid medium, **Materials and Corrosion,** 63, 7 (2012) 627-632**.**
52. J. John, S. Joseph, Electrochemical, quantum chemical, and molecular dynamic studies on the interaction of 4-amino-4H, 3,5-di(methoxy)-1,2,4-triazole (ATD), BATD, and DBATD on copper metal in 1N H_2SO_4, **Materials and Corrosion,** 647 (2013) 625-632.
53. H. L. Wang, H. B. Fan, J. S. Zheng, Corrosion inhibition of zinc in phosphoric acid solution by 2-mercaptobenzimidazole, **Material Chemistry and Physics,**77, 3 (2003) 655-661.
54. P. Zhao, Q. Liang, Y. Li, Electrochemical, SEM/EDS and quantum chemical study of phthalocyanines as corrosion inhibitors for mild steel in 1 mol/l HCl**, Applied Surface Science**, 2525, (2005)1596-1607.
55. V. S. Sastri, J. R. Perumareddi, Molecular orbital theoretical studies of some organic corrosion inhibitors, **Corrosion,** 538 (1997) 617-622.
56. F. E. Awe, S. O. Idris, M. Abdulwahab, E. E. Oguzie, Theoretical and experimental inhibitive properties of mild steel in HCl by ethanolic extract of Boscia senegalensis, **Cogent-Chemistry** (2015), doi.org/10.1080/23312009.2015.1112676.
57. Y. Zhou, X. Guo, X. Han, Corrosion Inhibition of Aluminium Anode by $CeCl_3$ in Simulated Seawater, **Advanced Materials Research**, 281 (2001) 11-16.
58. A. M. Ayuba, A. Uzairu, H. Abba, G. A. Shallangwa, Theoretical study of aspartic and glutamic acids as corrosion inhibitors on aluminium metal surface, **J. Mater. Environ. Sci**., 9, (2018), 3026-3034.
59. A. M. Al-Mayouf, A. A. Al-Suhybani, A. K Al-Ameery, Corrosion inhibition of 304SS in sulfuric acid solutions by 2-methyl benzoazole derivatives, **Desalination** 118 (1998), 25-23.